A Magnetic Micropump with Tri-membrane Fully Differential Structure

Lile Yu[a], Jingyun Xiao[b], Xingguo Xiong[a], Prabir Patra[b]

[a]*Department of Computer Engineering and Science, University of Bridgeport, CT, USA*

[b]*Department of Biomedical Engineering, University of Bridgeport, CT, USA*

***Abstract*—MEMS are typically defined as the devices or systems which are integrated with electrical and mechanical components on a silicon substrate through the microfabrication techniques. Due to its low cost, small size, low power consumption with high efficiency, MEMS technology has been widely used in many fields. In this paper, the design and simulation of a magnetic micropump with tri-membrane fully differential structure is presented. The proposed micropump has two inlets and two outlets. It has two pumping chambers sealed by three Si membranes. A permanent magnet is deposited on the middle membrane. Poly-Si coils are deposited on the top and bottom membranes separately. When electrical current is conducted in the coil, a magnetic field is excited, and its polarity (north and south poles) can be easily exchanged by reversing the conducting current. The design and analysis of the micropump has been discussed in details, and based on those theoretical analysis, a set of optimized design parameter has been achieved. The ANSYS simulation is used to verify the function of micropump. The proposed micropump leads to improved pumping rate with better efficiency.**

Keywords—ANSYS simulation, magnetic actuator, micropump, pumping rate,

I. INTRODUCTION

MEMS (Microelectromechanical Systems) micropumps are the pump devices with functional dimensions in micro that used to move around samples, reagents. It has been widely used in micro drug-delivery systems, Lab-on-a-chip (LOC) and many other bioMEMS applications for disease diagnosis and treatment [1].

Various micropump designs have been reported. Mechanical micropumps are classified as displacement type and dynamic type [2]. Displacement micropumps exert pressure forces on the working fluid is periodically to the point of overcoming channel and valve resistance. They include the pneumatic [3], thermopneumatic [4] and electrostatic micropumps [5]. Dynamic micropumps add mechanical energy continuously. Although dynamic micropumps do not get larger driving forces than the displacement micropumps, they caused less joule heat instead because of low voltage. The dynamic micropumps include acoustic micropumps(such as SAW) [6], surface tension based micropumps(such as EW) and electrokinematic micropumps (include EHD, MHD and DEP) [7]. Among those different kinds of micropump, magnetic micropumps have attracted strong interests. In [8], a rotating magnetic assembly actuator magnetic active-valve micropump is reported. It used peristaltic actuation principle, but they dimension the two valving chambers with a smaller depth than central pumping which can cause an increased backpressure of the pump. In [9], the reported micropump comprises of two PDMS layers, one permanent magnetic disc is deposited on the top layer with microvalves, another layer holding micro-ball valves and actuating chamber and an external magnet on the shaft of a small DC motor creates the serial membrane actuation. By controlling the rotation speed, the pumping rate can be adjusted. However, since a single membrane or single pump chamber is used, the pumping rate of the micropump is limited. In this research, a magnetic micropump with tri-membrane fully-differential structure is proposed. This proposed micropump is capable of delivering very high flow rate, and it can be easily controlled by conducting current.

II. DEVICE DESIGN

The structure design of the proposed bulk-micromachined magnetic micropump with tri-membrane fully differential structure is shown in Fig.1. This micropump has two pumping chambers sealed by three Si membranes. A permanent magnet is deposited on the middle membrane. Poly-Si coils are deposited on the top and bottom membranes separately.

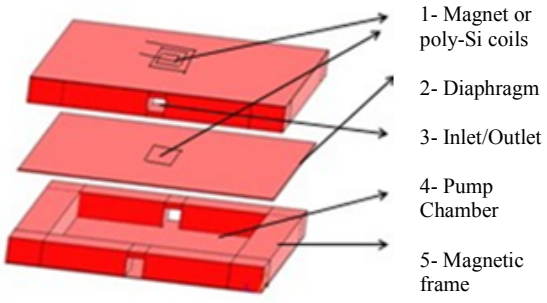

Fig1. Structure diagram of the magnetic tri-membrane micropump

III. WORKING PRINCIPLE

The working principle is explained as below. During the working mode, sinusoidal currents with equal amplitude and 180° phase difference are applied to top and bottom poly-Si coils, which excites magnetic fields with opposite polarities all

978-1-4799-5233-5/14/$31.00 ©2014 IEEE

the time. It shows in details in fig.3.The micropump works in two phases. In phase 1, the top membrane repels the magnet in middle membrane, and the bottom membrane attracts the magnet in middle membrane. As a result, the top chamber works in supply mode and the bottom chamber works in pump mode. In phase 2, the top membrane attracts the magnet in middle membrane, and the bottom membrane repels the magnet in middle membrane. As a results, the top chamber works in pump mode and the bottom chamber works in supply mode. By repeating this cycle, the top and bottom chambers pump out fluid alternately. Since each pump chamber has double membrane structure, this doubles the pumping rate compared to the traditional single-membrane design. The proposed micropump leads to improved pumping rate with better efficiency.

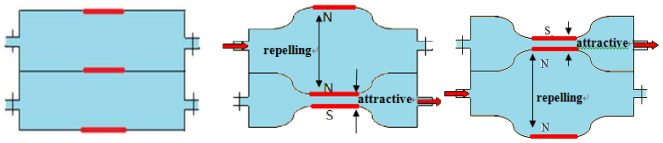

(a) Relaxed State

(b) Top chamber suck in bottom chamber pump out

(c) Top chamber pump out bottom chamber suck

Fig 2. Working principle of the tri-membrane micropump

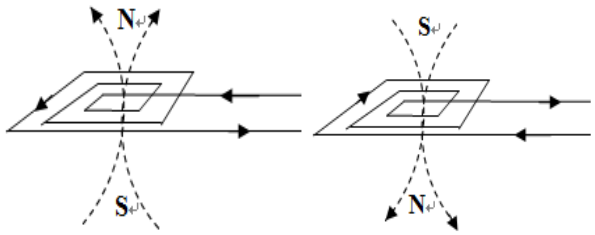

Fig 3. Control of north/south poles of electrical coil by switching the direction of current.

IV. ANALYSIS AND PERFORMANCE OF DESIGN

According to Maxwell equation, the pull force exerted by either an electromagnet or a permanent magnet at the "air gap" is define as

$$F = \frac{B^2 A}{2u_0} = \frac{(u_0 N_i / L)^2 A}{2u_0} = \frac{u_0 N_i^2 A}{2L^2} \tag{1}$$

In (1), F is force (SI unit Newton). A is the cross section of the area of the pole in square meters. B is the magnetic induction exerted by the magnet. U_0 is the permeability of space which equal $4\pi \times 10\text{-}7$ TM/A. N is the total number of turns. L is the length.

The magnetic force created by each coil is independent to the number of turns or the diameter of the wire used in coil. It depends on the current density <J>. Each coil will have the following current I.

$$I = \frac{<J> S_{spire}}{\alpha} \tag{2}$$

In (2), <J>: average current density inside the coil S_{spire}: copper surface of each spire α: proportion of the coil cross section occupied by the copper

Since we determine the maximum voltage is 9V for battery powered operation, and maximum current I is 200mA. We can get the dimension of the coil which are inner radius is 2 mm external radius is 9.5mm, thickness 2mm, $<J_{max}>$ is 1.25×107A/m-2. S_{spire} is 1.3×108 m2 and wire diameter t=0.135mm which is about 36-37 gauge wire. [10]
According to above analysis we assume the length of the magnet L = 40um, the width of the magnet W = 40um, then we can get

$$F = 226.08I^2 \tag{3}$$

For a square diaphragm (size: 2a×2a) under uniform pressure load p, in a coordinate system with origin in the center of the diaphragm, the bending displacement W(x,y) at any point (x,y) of the diaphragm can be calculated as

$$W_{(X,Y)} = 0.0213P\frac{a^4}{D}(1-\frac{x^2}{a^2})^2(1-\frac{y^2}{a^2})^2 \cong \frac{1}{47}P\frac{a^4}{D}(1-\frac{x^2}{a^2})^2(1-\frac{y^2}{a^2})^2 \tag{4}$$

Where:

$D = \frac{Eh^3}{12(1-v^2)}$
E: *Young's modulus* (*For Si*, $E = 1.7 \times 10^{11} pa$).
h: *the thickness of the diaphragm*
v: *Poisson's ratio* (*for Si*, $v = 0.34$)

According to (4), the maximum displacement is in the center of diaphragm [11-12]

$$W_{(0,0)} = \frac{1}{47} \mathrm{P} \frac{a^4}{D} \tag{5}$$

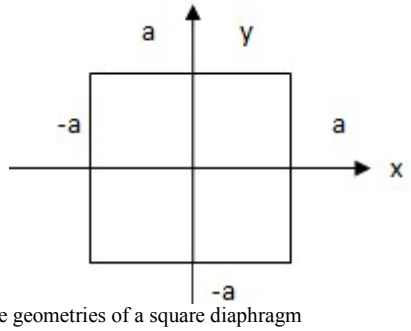

Fig 4. Structure geometries of a square diaphragm

Maximum displacement vs. thickness:

According to (4) and (5),

$$W_{max} = \frac{1}{47} Pa^4 \times \frac{12(1-v^2)}{Et^3} \tag{6}$$

The Si diaphragm having various edge length is simulated under a fixed load(1K Pa) on top surface and the result is shown below.

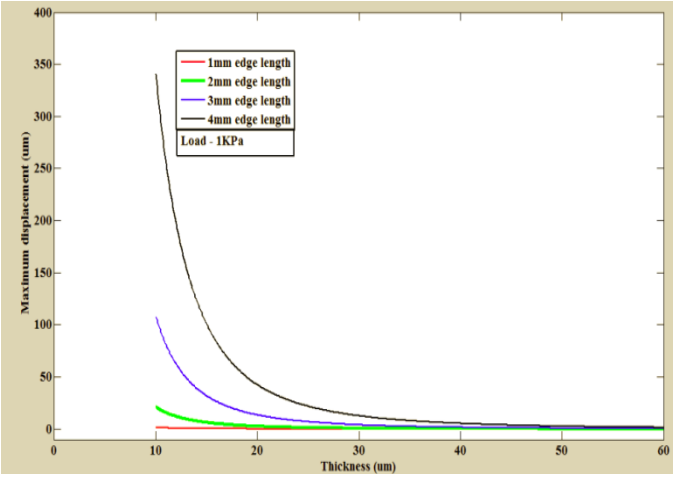

Fig 5. Maximum displacement vs. thickness characteristics of diaphragm

Above figure shows that as the thichness of the diaphragm is increased, the maximum diaplacement decreases for various edge length of the diaphragm. Morever, when the thickness of the diaphragm is doubled, the maximum deflection reduces by eight times.

Maximum displacement vs. edge length:

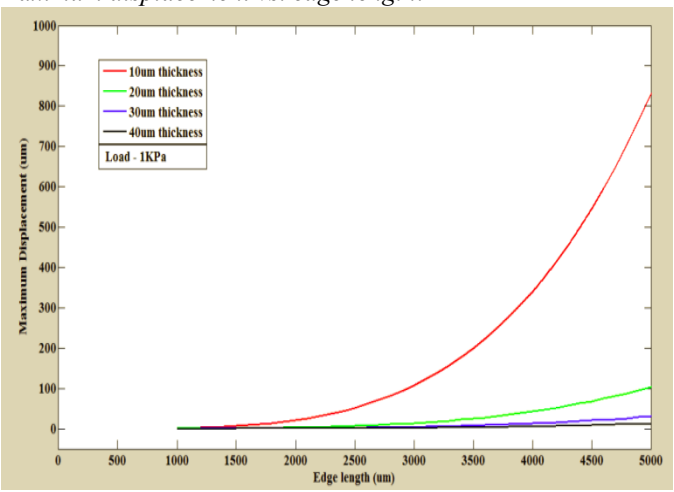

Fig 6. Maximum displacement vs. edge length characteristics of diaphragm

Fig.6 indicates that as the edge length of suqare diaphragm is increased, the maximum displacement also increased proportionally.

V. OPTIMIZATION

Based upon the above analysis, a set of optimized design parameters of the magnetic micropump is achieved. Some design parameters are shown in table1. The device has a dimension of 3.0mm ×3.0mm×0.82mm.

Table1. The optimized design parameters of the micropump

Design Parameters	Values
Length of pump (μm)	3000
Width of pump (μm)	3000
Height of pump (μm)	820
Length of magnet (μm)	400
Width of magnet (μm)	400
Thickness of magnet (μm)	60
Length of diaphragm (μm)	3000
Width of diaphragm (μm)	3000
Thickness of top and bottom diaphragm (μm)	40
Thickness of middle diaphragm (μm)	10
Length of inlet/outlet (μm)	400
Width of inlet/outlet (μm)	200
Thickness of inlet/outlet (μm)	200
Driving voltage (V)	9

Maximum bending displacement vs. coil current I:

As we determine the parameters of the design, The relationship between the maximum bending displacement Wmax of Si diaphragm and the coil current I is plotted in Fig.7, and it can be calculated as

$$W_{max} = 4.225I^2 \tag{7}$$

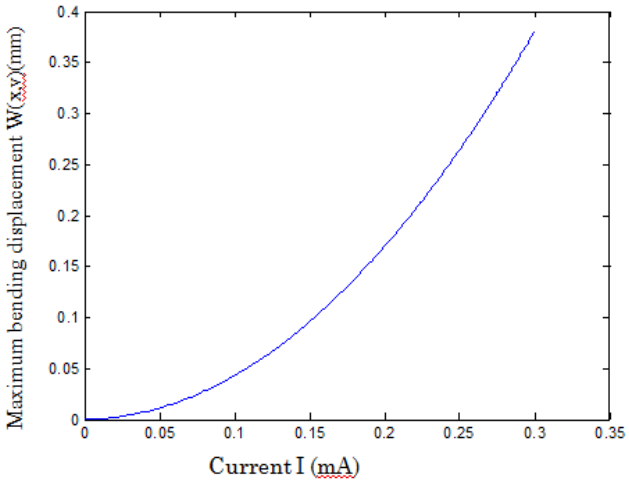

Fig 7. Maximum bending displacement of Si diaphragm v.s. coil current I

From the equation and figure we can see the more bending displacement of central Si diaphgram it is, the greater coil current it will be. Once the driving volatage increases, displacement also increases. Apart from this, The maximum bending displacement of central Si diaphragm is found to be 380μm, with the corresponding maximum coil current as 300 mA.

The 3D plot of bending shape of the Si diaphragm for coil current I = 300mA is shown in Fig.8. We can see that the maximum bending displacement occurs at the center of the diaphragm.

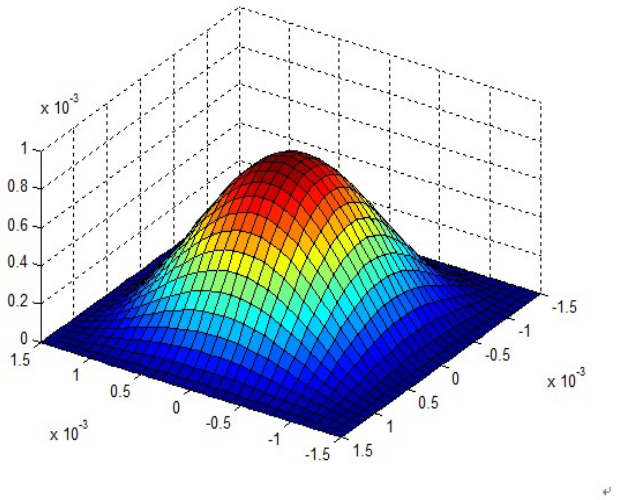

Fig 8. Bending shape of diaphragm

Flow rate of the micropump

The flow rate of the magnetic micropump can be calculated as

$$Q = 2\Delta V f \tag{8}$$

Where:

ΔV: *change volume of one diaphragm*

f: *frequency of diaphragm*

If we assume the pump shape is approximate as a sphere, one V is a spherical cap which is a portion of a sphere cut off by a plane. If the radius of the base of the cap is a, and the height of the cap is h, then volume of spherical cap can be calculated as:

$$V = \frac{\pi h}{6}(3a^2 + h^2) \tag{9}$$

Based on the equation above and optimized design parameters, we can get the change volume of one diaphragm in one cycle $\Delta V = 1.371 \times 10^{-6}$L, if we assume $f = 80$HZ, flow rate of magnetic micropump in one cycle $Q = 4.39 \times 10^{10}$pL/s.

VI. ANSYS SIMULATION

ANSYS is an engineering simulation software. It is used to solve mechanical problems such as static or dynamic structural analysis, and electro-magnetic problems. The dynamic analysis of this magnetic micropump predicts the relationship between device performance parameters and various design parameters (such as pump length, pump width, and pump thickness). However, those parameters are based on the theoretical analysis. In order to get a more accurate analysis for the design, ANSYS simulation is required to simulate the device resonant frequencies and other performance such as membrane displacement analysis.

By setting the displacement of surface of the device to be zero, we can do the resonant frequency simulation for the design. The first two vibration modes and the corresponding resonant frequency of each membrane of the micropump are shown in Fig. 9-11.

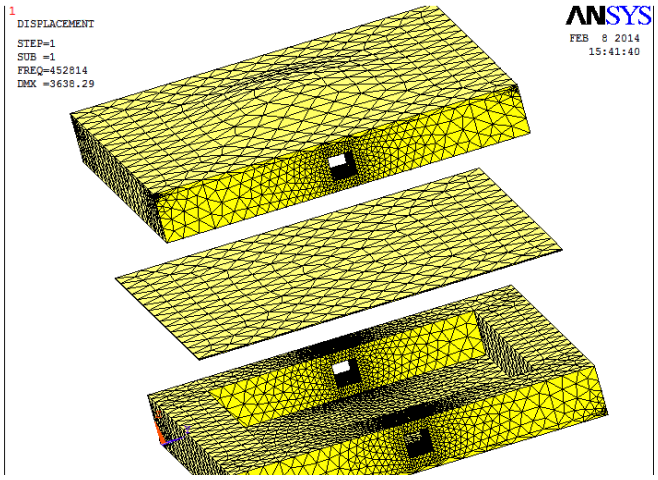

Fig 9. First vibration mode of top membrane of micropump (f_0=452814Hz)

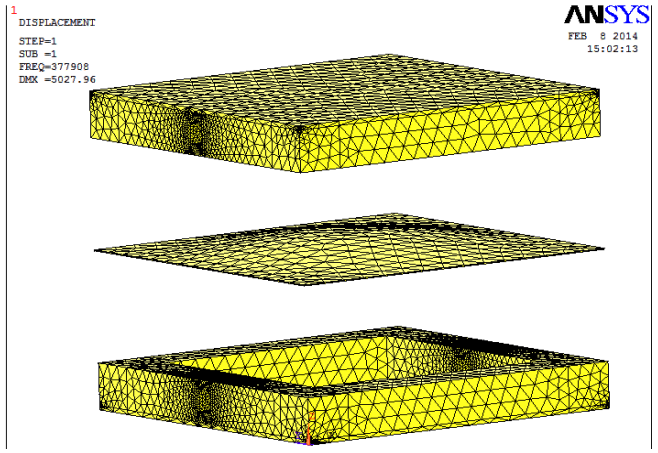

Fig 10. First vibration mode of middle membrane of micropump (f_0=377908Hz)

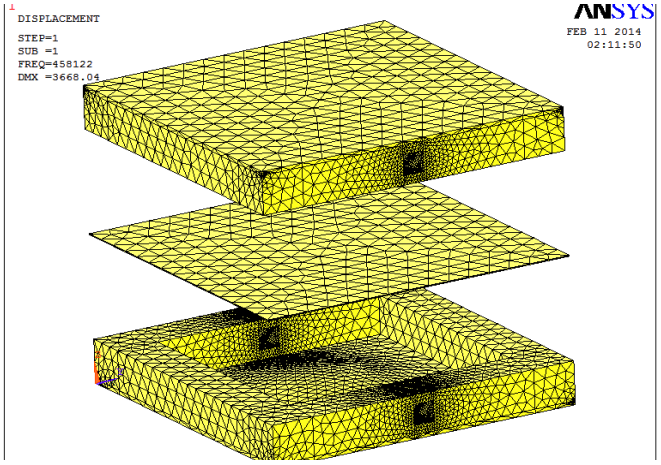

Fig 11. First vibration mode of bottom membrane of micropump (f_0=458122Hz)

Based on the ANSYS simulation, the resonant frequencies of the three membranes are close to each other, so that a fully differential actuation of the micropump can be achieved. Apart from this, the frequencies of second vibration are around 800000Hz which is far from first vibration, so that they will not interfere with each other. Those results can be very helpful for guiding future research and fabrication.

The stress contour plot of the Si membrane is shown in fig.12 Different parts of the model with different stress are shown with different colors, and parts of the model with blue color have a maximum stress. The maximum stress is 5027N/m^2 which is smaller than the material strength of Si (7000N/m^2), so that the membrane will not crack.

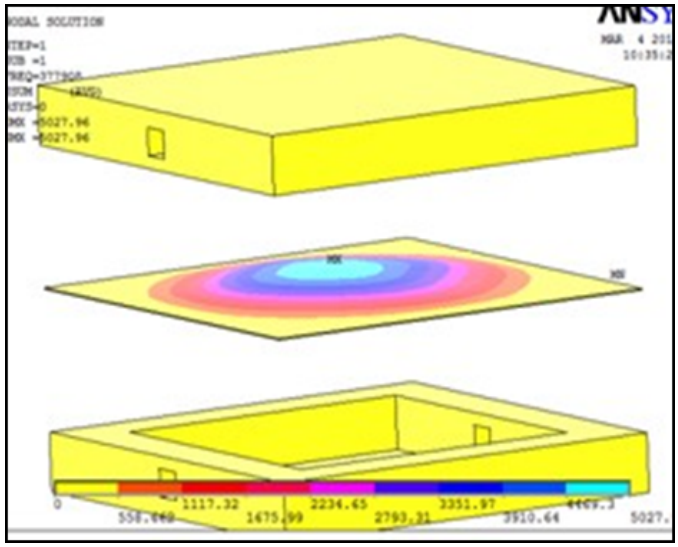

Fig 12. Stress contour plot of the central membrane

VII. FABRICATION

Generally, almost MEMS fabrication flows can be classified into two primary categories: bulk micromachining and surface micromachining. Bulk micromachining defines structure by selectively etching inside a substrate usually used silicon wafer as the substrate. Unlike bulk micromachining, surface micromachining create structure out of thin films on the top of the substrate. The magnetic tri-membrane micropump design in the research is fabricated with bulk micromachining process. The fabrication flow of the device is shown in Fig.13. All the structures are fabricated using Si KOH anisotropic etching. The fabrication steps are listed as follow. (1)Bare Si wafer; (2) double-face oxidation on Si wafer to form thin SiO2 layers; (3) photolithography to open window for inlet and outlet; (4) KOH wet etching to form the inlet and outlet; (5) remove all SiO_2 and re-oxide to get 1.0 um SiO_2.(6) photolithography to open window for Si membrane;(7) KOH wet etching to get Si membrane (8) deposit Poly-Si or magnet material; (9) Photolithography plus etching to pattern poly-Si coils or magnet material; (10) repeat for other two parts; (11) to bond all these three parts; (12) device fabrication completed. During the bonding process, precise alignment is required to ensure the proper function of the device

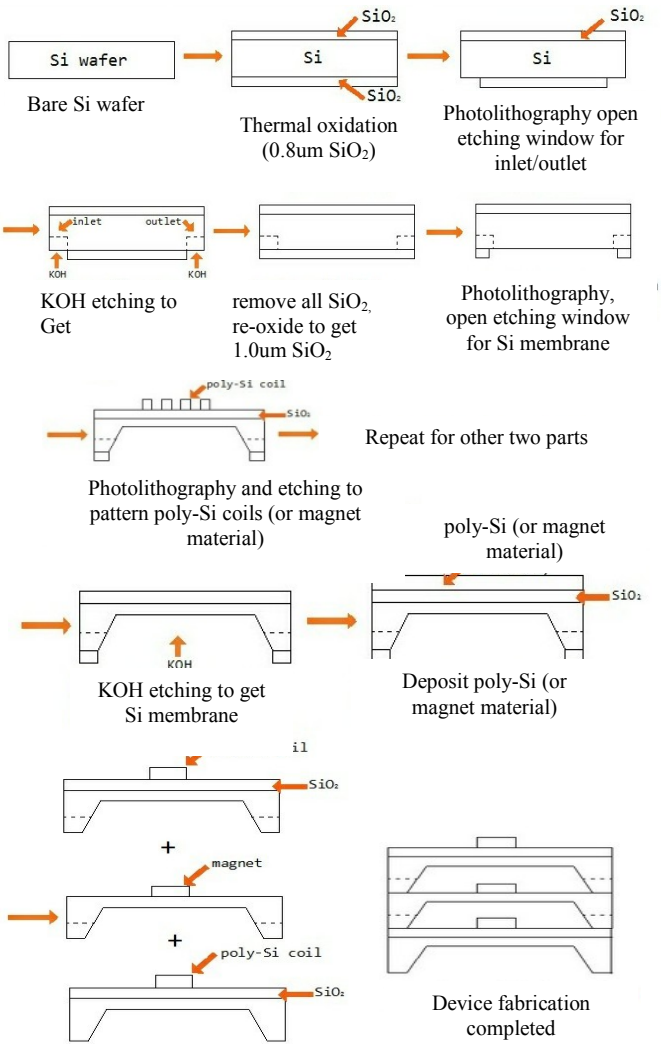

Fig 13. Fabrication flow of the micropump (cross-sectional view)

VIII. CONCLUSION

In this paper, a magnetic micropump with tri-membrane fully differential structure is proposed. The working principle of the micropump is analyzed in details. Based on the analysis, an optimized design of the micropump is suggested. ANSYS simulation is used to verify the correct function and performance of the device. The fabrication process of the device is also proposed. Theoretical calculation shows that he pumping rate of magnetic micropump in one cycle $Q = 4.39 \times 10^{10} pL/s$. The proposed micropump can be used for various biomedical applications with the high performance.

In the future, we will continue to improve the device design, such as reversing the pumping flow, in addition, we also can do the further work to analysis other function of this design such as pumping different microfluid in one time.

REFERENCE

[1] Jeremy A. Walraven, "Introduction to applications and industries for microelectromechanical system (MEMS)" Test conference 2003, PP.674-680.

[2] Ho-Jin Kang, Bumkyoo Choi, "Development of the MHD micropump with mixing function" Sensors and Actuators A 165 (2011), PP. 439-445.

[3] Oana Tatiana Nedelcu, Jean-Luc Morelle, Catalin Tibeica, Samuel Voccia, Irina Codreanu, Severin Dahms, "Modelling and Simulation of a Pneumatically Actuated Micropump" Semiconductor Conference, 2007, PP. 77-80

[4] Bonnie Tingting Chia, Hsin-Hung Liao, Yao-Joe Yang, "A Novel Thermo-pnematic Peristaltic Micropump with Low Temperature Elevation" Solid-State Sensors, Actuators and Microsystems Conference, 2009, PP. 2286-2289.

[5] Wen-yao Liu, "Research on Electrostatic Micropump Pull-in Phenomena Based on Reduced Order Model" Intelligent Computation Technology and Automation Conference, 2010, PP.1154-1157

[6] Y.Q. Fu, X.Y. Du etc, "SAW Streaming in ZnO Surface Acoustic Wave Micromixer and Micropump" IEEE SENSORS Conference, 2007, PP. 478-483.

[7] M. Tanski, M. Kocik, J. Mizeraczyk, "Liquid Pumping by Miniature ElectroHydrodynamic Pump Driven by DC Voltage" IEEE International Conference on Dielectric Liquids, 2011

[8] M.Shen, L.Dovat, M.A.M. Gijs, "Magnetic active-valve micropump actuated by a rotating magnetic assembly" Sensors and Actuators B, 2011, PP.52-58.

[9] Scott McDonald, Tingrui Pan, and Babak Ziaie, "A Magnetically Driven PDMS Micropump with Micro-Ball Valves" Engineering in Medicine and Biology Society, 2004, 26th Annual International Conference of the IEEE, PP 2650-2653

[10] Mattew L. Cantwell, Farid Amirouche, Johann Citerin, "Low-cost high performance disposable micropump for fluidic delivery" Sensors and Actuators A 168 (2011), pp. 187-194

[11] Souvik Sutradhar , "Optimization of geometry of microfabricated piezoelectric actuator" International journal of engineering trends and technology(IJETT), Volume4, April 2013, PP 580-585.

[12] Nadim Maluf, Kirt Williams, "An Introduction to Microelectromechanical Systems Engineering", 2nd Edition, Artech House, 2004, ISBN: 1580535909